JOURNAL OF MATERIALS SCIENCE 29 (1994) 3949–3954

Effect of grain morphology and grain size on the mechanical properties of Al_2O_3 ceramics

TAKASHI KOYAMA, AKIO NISHIYAMA
Central Research Institute, Mitsubishi Materials Corporation, 1-297 Kitabukuro-cho, Omiya, Saitama 330, Japan

KOICHI NIIHARA
The Institute of Scientific and Industrial Research (ISIR), Osaka University, 8-1 Mihogaoka, Ibaraki, Osaka 567, Japan

Bending strength, fracture toughness, fracture energy and crack extension resistance were evaluated for Al_2O_3 ceramics with equi-axed and platelet grains. Bending strength was proportional to grain size$^{-1/2}$, but flaws with a size of 10 μm controlled the strength when the microstructure was finer than 10 μm. Fracture toughness, measured by the single etched precracked beam (SEPB) method, was proportional to fracture energy$^{1/2}$, and increased with the grain size of Al_2O_3 ceramics with equi-axed and platelet grains. However, the toughness of platelet grain ceramics was higher than the ceramics with equi-axed grains, and increased up to 6.6 MPa m$^{1/2}$ with grain size. Therefore, it is thought that fracture toughness not only depends on grain size, but also on grain morphology; equations were derived to account for this phenomenon.

1. Introduction

It has been reported that the crack resistance of Al_2O_3 ceramics increases with crack propagation [1, 2], and this behaviour (*R*-curve) becomes remarkable when the grain size increases [3]. As a result, the fracture toughness, measured by the single etched precracked beam (SEPB) method, and fracture energy increase with grain size [3]. This *R*-curve behaviour of Al_2O_3 ceramics is due to grain bridging and grain pullout, and were identified by optical microscopy and scanning electron optical microscopy [4–7]. These toughening mechanisms have also been widely reported in silicon nitride ceramics and whisker reinforced ceramics. In these ceramics, the effect of microstructure (e.g. grain diameter, grain length and aspect ratio) on fracture toughness has been reported in some papers, and it has been found that the toughness depends on the radius of bridging microstructural features; these bridging microstructural features were large grains in silicon nitride ceramics [8] and whiskers in whisker reinforced ceramics [9].

Recently the effect of dopants on the sintering behaviour of Al_2O_3 ceramics has been clearly understood, which permits control over the microstructure. For example, $Na_2O + SiO_2$, $CaO + SiO_2$, $SrO + SiO_2$, or $BaO + SiO_2$ dopants react with Al_2O_3 to produce a liquid phase during sintering, which results in elongated platelike or platelet grains [10].

In the present study, Al_2O_3 ceramics with equi-axed and platelet grains were produced by the addition of small amounts of $CaO + SiO_2$ [11]. The effects of grain morphology and grain size on the mechanical properties, bending strength, fracture toughness, fracture energy and crack extension resistance, were investigated.

2. Experimental procedure

2.1. Materials

The mechanical properties of Al_2O_3 ceramics with equi-axed and platelet grains were measured. To obtain Al_2O_3 ceramics with equi-axed grains, undoped Al_2O_3 compacts were sintered at 1300–1600 °C for 4 h in air and 1600–1800 °C for 4 h in Ar gas. Al_2O_3 compacts doped with 0.02–0.25 mol% $CaO + SiO_2$ were sintered at 1500–1600 °C for 4 h in air to obtain ceramics with platelet grains. The grain size of Al_2O_3 ceramics with equi-axed grains was obtained by a linear-intercept method, and the size of platelet grains was calculated from the equation derived by Fullman [12]. It was assumed that the platelet grains were circular in shape; for each sample the size of about 100 grains was measured to obtain diameter, H, thickness, T, and aspect ratio, H/T.

Fig. 1 shows the typical microstructure of Al_2O_3 ceramics. Undoped Al_2O_3 ceramics had equi-axed grains, which increased in size with sintering temperature. Ceramics with 0.02 mol% $CaO + SiO_2$ had platelet grains with relatively small grain sizes, but the platelet grains grew larger when the content of dopants increased.

2.2. Measurement of mechanical properties

Bending strength was measured using the three-point bending test (JIS *R*-1601). The specimens were 3 × 4

0022–2461

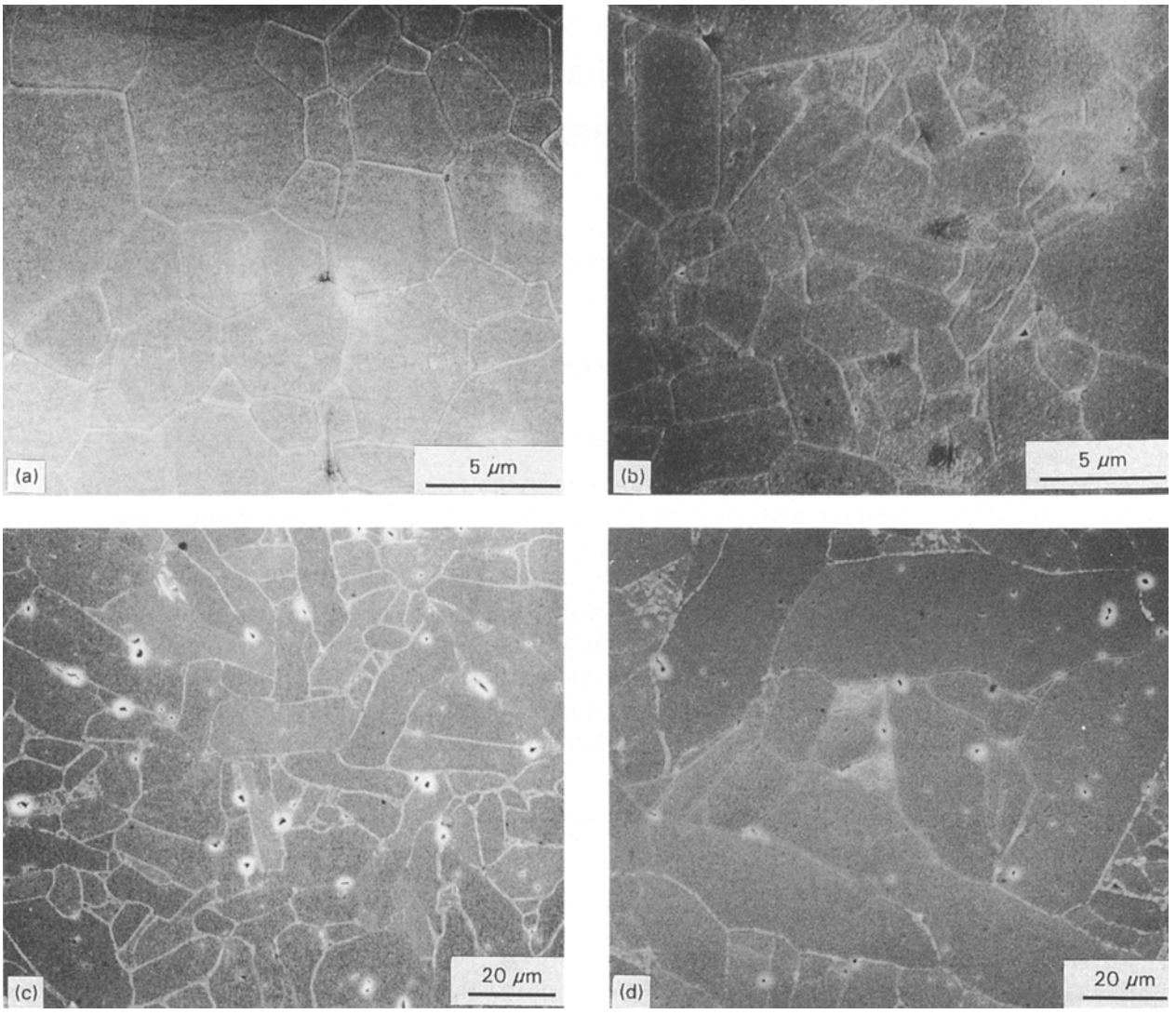

Figure 1 Typical microstructure of Al_2O_3 ceramics used in this experiment: (a) undoped Al_2O_3 sintered at 1500 °C; (b) Al_2O_3 + 0.02 mol% CaO + 0.02 mol% SiO_2 sintered at 1600 °C; (c) Al_2O_3 + 0.25 mol% CaO + 0.25 mol% SiO_2 sintered at 1500 °C; and (d) Al_2O_3 + 0.05 mol% CaO + 0.05 mol% SiO_2 sintered at 1600 °C.

× 40 mm, and the span was 30 mm. Fracture toughness, K, was measured by the single etched precracked beam (SEPB) method (JIS *R*-1607) [13]; and Young's modulus, E, was measured by the resonance–vibration method in bending geometry (JIS *R*-1602). Fracture energy, γ, and crack extension resistance, K_R, were evaluated from the stably fractured load–displacement curve of the bending bar with chevron notch (CN). Fracture energy was calculated from the areas under the load–displacement curves and respective ligament areas [14]. Characteristic between crack resistance and crack length were obtained from the same load–displacement curve analysed by the compliance model [15]. The compliance was calculated by Bluhm's slice model. To observe the manner of fracture, the fracture surfaces and the pop-in cracks for the measurement of toughness were examined by scanning electron microprobe.

3. Results and discussion

3.1. Bending strength

Fig. 2 shows the effect of grain size on the bending strength of Al_2O_3 ceramics. The grain size of Al_2O_3 ceramics, with equi-axed grains, was the value measured by the linear-intercept method, and the size of the ceramics with platelet grains was the diameter of platelet grains. The strength showed the Orowan–Petch relationship; the bending strength for large grains was proportional to grain size$^{-1/2}$, and the strength was nearly constant for ceramics with a grain size below 10 μm. In general, strength was proportional to flaw size$^{-1/2}$, and flaws changed from intrinsic flaws to extrinsic flaw as the grain size decreased. In the case of Al_2O_3 ceramics, residual stress was generated by thermal expansion anisotropy, and produced intrinsic flaws where size was proportional to the grain size. However, Chantikul *et al.* [16] investigated the interrelationships between strength and grain size, and reported that the strength was a complex function of both flaw size and grain size, and that the extrinsic flaw size was about 10 μm. Some researchers produced Al_2O_3 ceramics using slip casting and hot isostatic pressing in order to minimize these extrinsic flaws, but higher strength could not be obtained [17]. Therefore, the formation of these ex-

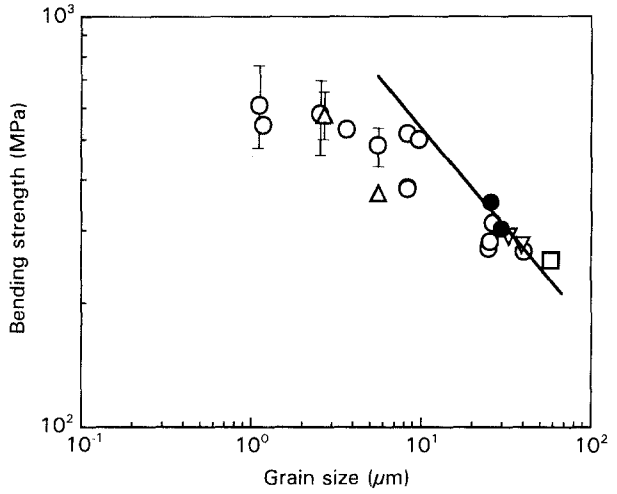

Figure 2 Influence of grain size on the bending strength of Al_2O_3 ceramics. Line indicates the calculated value obtained by the equation $\sigma = KY^{-1}C^{-1/2}$, where C is the flaw size. It is assumed that the flaw size is equal to the grain size and $K = 3$ MPa $m^{1/2}$. (○) 0 mol%, (△) 0.02 mol%, (□) 0.05 mol%, (▽) 0.15 mol%, (●) 0.25 mol%.

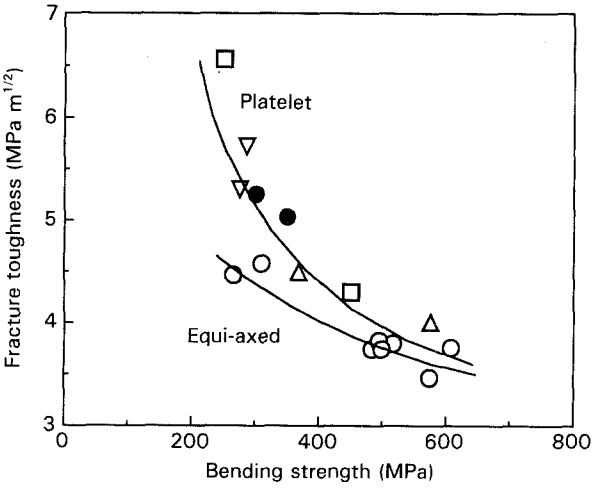

Figure 3 Relationship between fracture toughness and bending strength: (○) 0 mol%, (△) 0.02 mol%, (□) 0.05 mol%, (▽) 0.15 mol%, (●) 0.25 mol%.

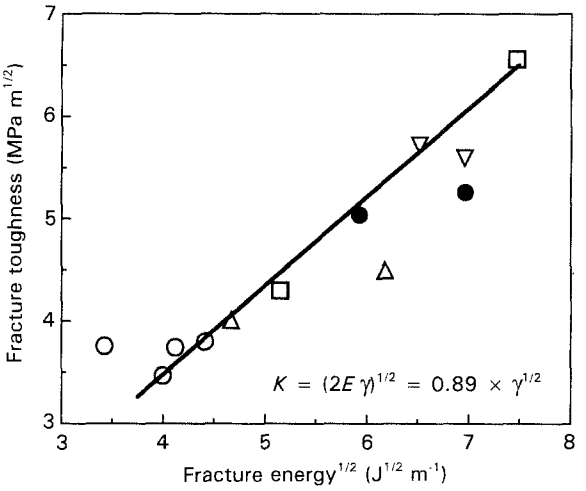

Figure 4 Relationship between fracture toughness, K, and fracture energy, γ. Line indicates the calculated value obtained by the equation $K = (2E\gamma)^{1/2}$, where E is Young's modulus: (○) 0 mol%, (△) 0.02 mol%, (□) 0.05 mol%, (▽) 0.15 mol%, (●) 0.25 mol%.

trinsic flaws were thought to be due to pores or to the inhomogeneity of the microstrucutre, which were difficult to eliminate.

3.2. Fracture toughness and fracture energy

The relationship between bending strength and fracture toughness measured by the SEPB method is shown in Fig. 3. Fracture toughness increased as the bending strength decreased, and doped Al_2O_3 ceramics with platelet grains had higher toughness. The relationship between fracture toughness and fracture energy measured using CN bars is shown in Fig. 4. Fracture toughness was proportional to fracture energy$^{1/2}$, and this relationship could be explained from the equation $K = (2E\gamma)^{1/2}$, because the Young's modulus of all Al_2O_3 ceramics was about 390 GPa. Since the fracture energy was obtained from the measurement of the stably fractured load–displacement curve, the fracture toughness measured by the SEPB method did not yield the same value as when the crack was initiated.

Typical fracture surfaces and crack paths are shown in Fig. 5. These cracks were the pop-in cracks used for the measurement of fracture toughness by the SEPB method. Al_2O_3 ceramics with equi-axed grains had low toughness, and these ceramics fractured intergranularly. The width of the crack's propagating zone was only about 5 μm, though the pop-in crack propagated along the grain boundary. On the other hand, Al_2O_3 ceramics with platelet grains had higher toughness, and the width of the crack's propagating zone was 10–20 μm for the ceramics. It was observed that grain bridging was accompanied by crack branching and crack deflection, and that these ceramics fractured transgranularly. According to the direct observation of crack paths, all the grains along the trace did not bridge the crack, and the mean spacing of the grain bridging site was about 2–5 grain diameters. Nishida and Kameyama [3] reported that rough fracture surfaces occurred in the case of tough ceramics, and that this made the interaction between fracture surfaces larger. The anisotropy of thermal expansion caused residual stress in the Al_2O_3 ceramics, and this stress became larger and more inhomogeneous as the grain size increased. Since cracks propagated at easily fractured surfaces which were weak or stressed in a tensile manner, the fracture surfaces became rough when the grain size increased. These rough surfaces became obstacles for further fracture, and secondary fracture and friction occurred before the specimen was fractured completely.

It was considered that this improvement of fracture toughness could be due not only to grain growth, but also to the presence of an intergranular glassy phase. Padture and Chan [18] added 1 vol% anorthsite glass to Al_2O_3 ceramics and crystallized the glass to generate residual stress between the Al_2O_3 matrix and the intergranular phase, which improved the flaw tolerance and fracture toughness. In this research, however the effect of the intergranular phase on the mechanical

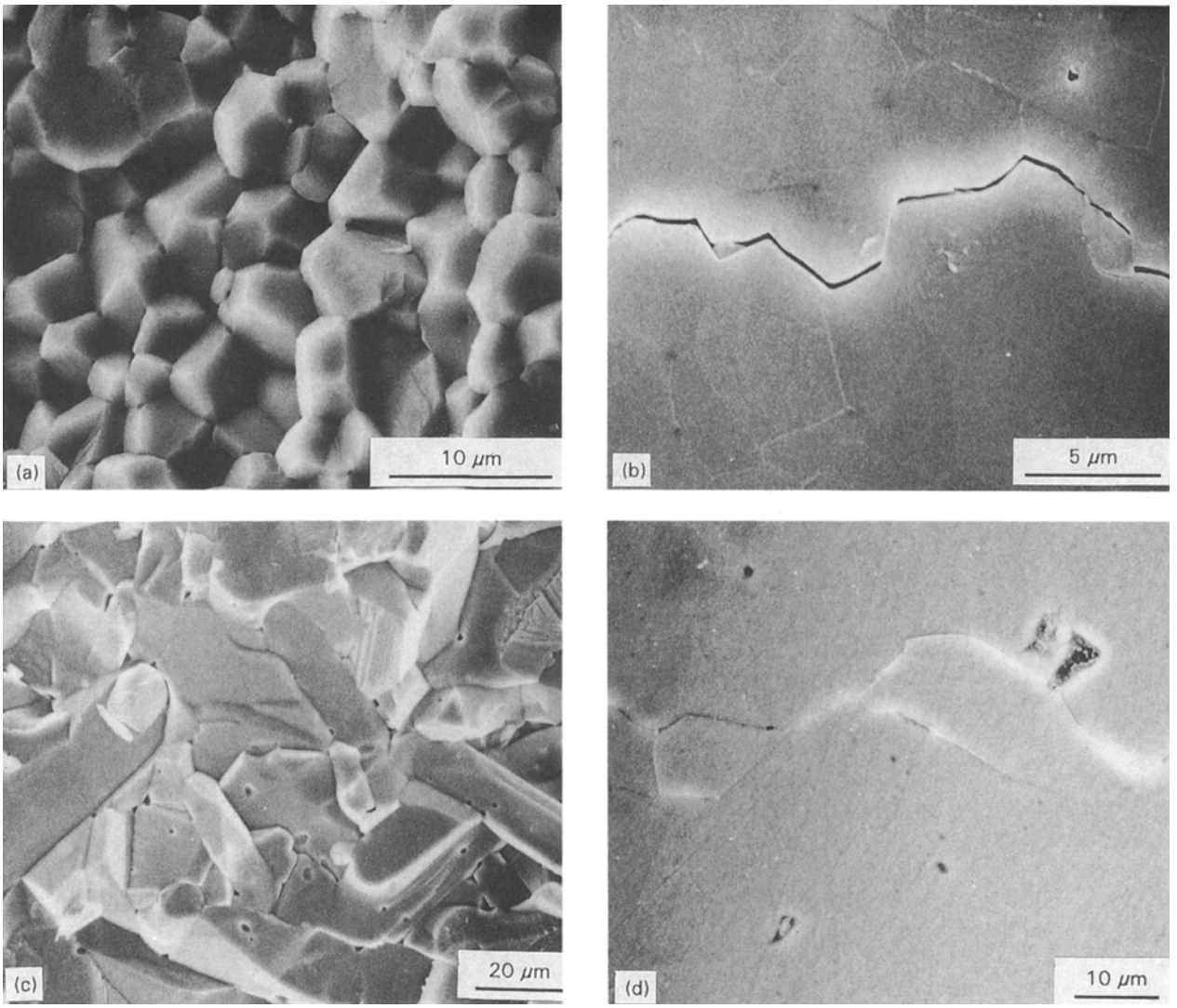

Figure 5 Typical fracture surfaces and crack paths of Al_2O_3 ceramics with equi-axed grains and platelet grains. These cracks were pop-in cracks for the measurement of fracture toughness by the SEPB method.

properties was not taken into consideration, since the intergranular phase, which had a maximum content of only 0.6 vol% for 0.25 mol% doped Al_2O_3 ceramics, was not crystallized and a relationship between the content of dopants and the fracture toughness was not to be found. Hence only the effects of grain morphology and grain size on the fracture toughness of Al_2O_3 ceramics have been discussed.

It is known that the fracture toughness and fracture energy of anisotropic materials, like Al_2O_3 ceramics, can be improved by grain growth, since crack bridging occurs due to large grains which cause compressional stresses by thermal expansion anisotropy. Vekinis *et al.* [4] reported that these stresses were the result of both grain morphology and thermal expansion anisotropy, and they made some simple models to investigate the effect of grain size on the fracture energy. Modifying their equation for pullout, assuming the shape of platelet grains with diameter, H, and thickness, T, is simplified into square plates of size $[(\pi/2)/2 \times H] \times [(\pi/2)/2 \times H] \times T$ with the same volume. During pullout, work is done on these grains against friction, which occurs effectively on the plates from $[(\pi/2)/2 \times H]$ to $(1 - X)[(\pi/2)/2 \times H]$ and does not occur when the crack opens beyond $X[(\pi/2)/2 \times H]$. Then

$$\Delta\gamma = \pi^{2/3}(1 - X)^2 N_a \mu \sigma_a H^3/16 \quad (1)$$

where N_a is the number of bridging grains per unit area, μ is the friction coefficient, and σ_a is the pullout stress. Since the relationship between the fracture toughness and the fracture energy is $K = (2E\gamma)^{1/2}$ and $\gamma \gg \gamma_o$, then

$$K = (2E\gamma)^{1/2} = (2E\gamma_0 + 2E\Delta\gamma)^{1/2}$$

$$\fallingdotseq (2E\gamma_0)^{1/2} + (2E\Delta\gamma)^{1/2} \fallingdotseq K_0 + \Delta K \quad (2)$$

Setting $N_a = f(\pi H^2 T/4)^{-2/3}$, where f is the ratio of grains acting pullout, then

$$\Delta K \fallingdotseq (2E\Delta\gamma)^{1/2}$$

$$= \pi^{3/4} 2^{-3/2} (1-X)(f\mu\sigma_a E)^{1/2} H^{5/6} T^{-1/3} \quad (3)$$

$$= \pi^{3/4} 2^{-3/2} (1-X)(f\mu\sigma_a E)^{1/2} (H/T)^{1/3} H^{1/2} \quad (4)$$

$$= \pi^{3/4} 2^{-3/2} (1-X)(f\mu\sigma_a E)^{1/2} (H/T)^{5/6} T^{1/2} \quad (5)$$

This equation shows that fracture toughness is proportional to diameter$^{5/6}$, thickness$^{-1/3}$, and toughness is proportional to both diameter$^{1/2}$ and thickness$^{1/2}$ for ceramics with the same aspect ratio, H/T. Fig. 6

shows the dependence of fracture toughness of Al_2O_3 ceramics on diameter$^{1/2}$, thickness$^{1/2}$ and diameter$^{5/6}$ thickness$^{-1/3}$. The fracture toughness increased with both diameter and thickness, but the slope was the same only for the relationship between the toughness and diameter$^{5/6}$ thickness$^{-1/3}$. The real bridging stress, σ, can be calculated by use of the equation

$$\sigma = N_a(2\mu\sigma_a)[(\pi/2)^{1/2} \times H]^2$$
$$= (2\pi)^{1/3} f\mu\sigma_a(H/T)^{2/3} \quad (6)$$

The bridging stress, σ, reported by several researchers was 30–70 MPa [18, 19]. Taking $\sigma = 50$ MPa, $H/T = 4.5$, and $E = 390$ GPa in Equations 3 and 6, $f\mu\sigma_a = 10$ MPa and $X = 0.85$ can be obtained using the slope between the fracture toughness and diameter$^{5/6}$ thickness$^{-1/3}$ in Fig. 6. Bridging does not occur when the crack opens beyond $X[(\pi/2)/2 \times H]$ and the maximum crack opening displacement, $(1-X)[(\pi/2)/2 \times H]$, is $0.13H$. This value is a little lower than the crack opening displacement, $D/4$, reported by several researchers [19, 20], because they represented the grain size using only the grain diameter, D. Since

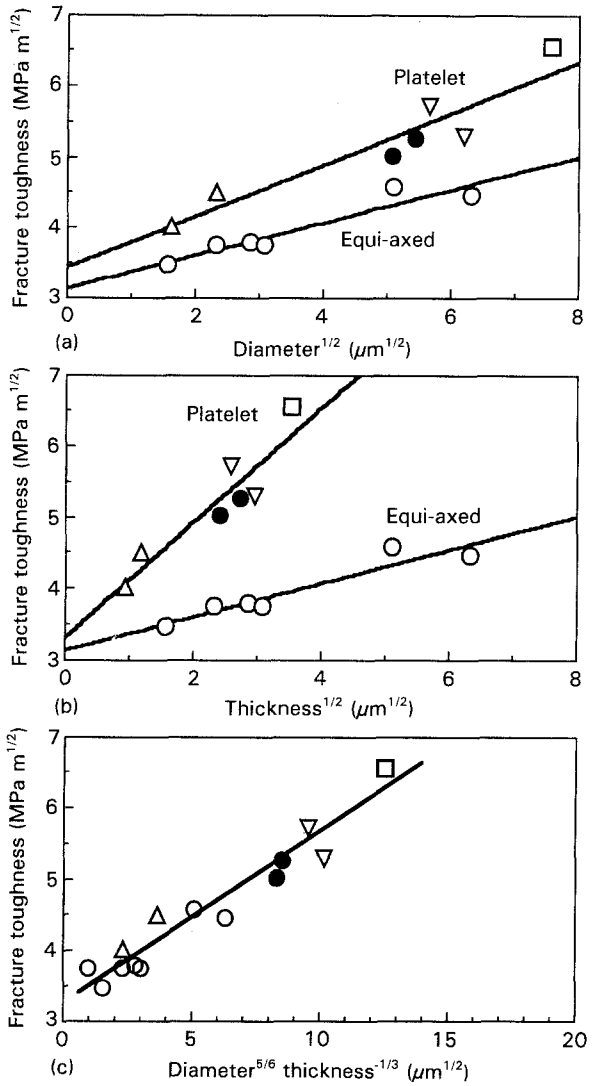

Figure 6 Fracture toughness of Al_2O_3 ceramics as a function of (a) diameter$^{1/2}$, (b) thickness$^{1/2}$ and (c) diameter$^{5/6}$ thickness$^{-1/3}$: (○) 0 mol%, (△) 0.02 mol%, (□) 0.05 mol%, (▽) 0.15 mol%, (●) 0.25 mol%.

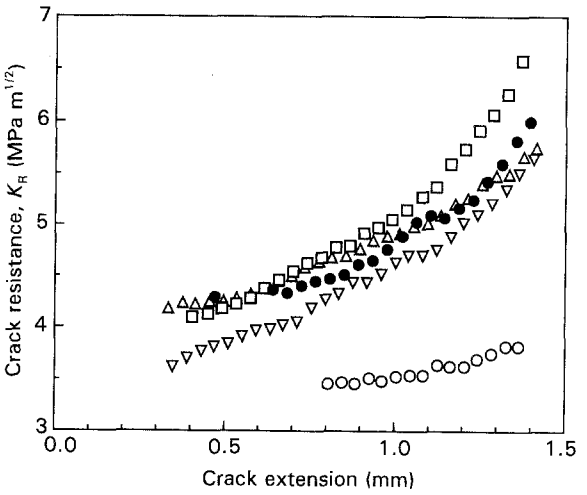

Figure 7 Crack extension resistance of Al_2O_3 ceramics. Al_2O_3 ceramics doped with 0–0.25 mol% CaO + SiO_2 were sintered at 1600 °C: (○) 0 mol%, (△) 0.02 mol%, (□) 0.05 mol%, (▽) 0.15 mol%, (●) 0.25 mol%.

$D^3 = \pi H^2 T/4$ and $H/T = 4.5$, the crack opening displacement is $0.23D$ which is close to $D/4$.

Consequently, the effect of grain morphology and grain size on the fracture toughness of Al_2O_3 ceramics could be explained, and equations were derived on the basis of grain pullout model.

3.3. Crack resistance

The crack resistance of Al_2O_3 ceramics sintered at 1600 °C is shown in Fig. 7. Crack length calculated from the change of compliance was the length from the top of the chevron notch. Al_2O_3 ceramics with larger platelet grains, which had higher fracture toughness, indicated larger R-curve characteristics than the ceramics with equi-axed grains. However, the initial value of crack resistance and the plateau of the R-curve could not be obtained, probably because the compliance calculated from the geometry of the specimen was not exact and because the chevron notch was used. Upon exposing these curves to the crack initiation value, 3–4 MPa m$^{1/2}$ was obtained and this value was independent of grain size.

4. Conclusions

Bending strength, fracture toughness, K, fracture energy, γ, and crack extension resistance were evaluated for Al_2O_3 ceramics with equi-axed and platelet grains. The results are summarized as follows:

1. Bending strength was proportional to grain size$^{-1/2}$, but flaws with a size of 10 μm controlled the strength when the grain size was less than 10 μm.

2. The fracture toughness measured by the single etched precracked beam (SEPB) method was proportional to fracture energy$^{1/2}$; this relationship could be explained from the equation $K = (2E\gamma)^{1/2}$.

3. The fracture toughness of Al_2O_3 ceramics with equi-axed and platelet grains increased with grain size,

but the toughness of ceramics with platelet grains was higher and increased up to 6.6 $MPam^{1/2}$ with grain size. Therefore, it was thought that fracture toughness depended not only on the grain size, but also on grain morphology. Equations for toughness were derived which included grain diameter, thickness and aspect ratio.

4. Al_2O_3 ceramics with large platelet grains, which had higher fracture toughness, indicated larger *R*-curve characteristics than ceramics with equi-axed grains.

Acknowledgements

We are indebted to Dr Giuseppe Pezzotti (Toyohashi University of Technology, Japan) and Dr Kenichi Matsushita (Osaka University, Japan) for help in the measurement of crack extension resistance and Young's modulus.

References

1. R. STEINBRENCH, R. KNEHANS and W. SCHAARWÄCHTER, *J. Mater. Sci.* **18** (1983) 265.
2. M. V. SWAIN, *J. Mater. Sci. Lett.* **5** (1986) 1313.
3. T. NISHIDA and I. KAMEYAMA, *J. Ceram. Soc. Jpn* **100** (1992) 276.
4. G. VEKINIS, M. F. ASHBY and P. W. R. BEAUMONT, *Acta Metall. Mater.* **38** (1990) 1151.
5. J. RÖDEL, J. F. KELLY and B. R. LAWN, *J. Amer. Ceram. Soc.* **73** (1990) 3313.
6. P. L. SWANSON, C. J. FAIRBANKS, B. R. LAWN, Y-M. MAI and B. J. HOCKEY, *ibid.* **70** (1987) 279.
7. R. F. COOK, *Acta Metall. Mater.* **38** (1990) 1083.
8. T. KAWASHIMA, H. OKAMOTO H. YAMAMOTO and A. KITAMURA, *J. Ceram. Soc. Jpn* **99** (1991) 320.
9. P. F. BECHER, C-H. HSUEH, P. ANGELINI and T. N. TIEGS, *J. Amer. Ceram. Soc.* **71** (1988) 1050.
10. H. SONG and R. L. COBLE, *ibid.* **73** (1990) 2077.
11. T. KOYAMA, A. NISHIYAMA and K. NIIHARA, *J. Mater. Sci.* **28** (1993) 5953.
12. R. L. FULLMAN, *Trans. AIME* **197** (1953) 447.
13. T. NOSE and T. FUJII, *J. Amer. Ceram. Soc.* **71** (1988) 328.
14. J. NAKAYAMA, *ibid.* **48** (1965) 583.
15. J. I. BLUHM, *Eng. Fract. Mech.* **7** (1975) 593.
16. P. CHANTIKUL, S. J. BENNISON and E. R. LAWN, *J. Amer. Ceram. Soc.* **73** (1990) 2419.
17. H. MIZUTA, K. ODA, Y. SHIBASAKI, M. MAEDA, M. MACHIDA and K. OHSHIMA, *ibid.* **75** (1992) 469.
18. N. P. PADTURE and H. M. CHAN, *ibid.* **75** (1992) 1870.
19. A. REICHL and R. W. STEINBRECH, *ibid.* **71** (1988) C299.
20. X-Z. HU, E. H. LUTZ and M. V. SWAIN, *ibid.* **74** (1991) 1828.

Received 2 August 1993
and accepted 28 January 1994